Effects of Structure Parameters and Structural Deviations on the Characteristics of Photonic Crystal Directional Couplers

Xiaoyu Mao, Yidong Huang, *Member, IEEE*, Kaiyu Cui, Chao Zhang, Wei Zhang, and Jiangde Peng

***Abstract*—The effects of structure parameters and structural deviations on the characteristics of photonic crystal directional couplers (PCDCs) were analyzed through a systematic simulation study. The relationship between coupling characteristics and structure parameters was discussed. The results reveal that the remained power in the coupling region is detrimental to reducing the insertion loss of PCDCs, especially for the PCDCs with shorter coupling length. An improved structure, which increases the radii of air holes in the post coupling region, was proposed to suppress the remained power and reduce the insertion loss effectively. The influence of structural deviations, which is caused by fabrication imperfections and results in the mismatch between experimental results and theoretical predictions, was also investigated using statistical methods. The simulation results show that the air hole position misalignment perpendicular to the waveguide direction has the largest effect on the insertion loss of PCDCs, and reducing r/a is helpful to improving the robustness of PCDCs.**

***Index Terms*—Couplers, photonic crystals, structural deviations, structure parameters.**

I. Introduction

TWO-dimensional photonic crystal waveguide (2-D PCWG) has a great advantage over the conventional optical waveguide by total internal reflection because it is possible to realize sharp waveguide bends with low losses [1], [2]. So it has been expected to realize optical integrated circuits with ultrasmall size [3], [4].

Photonic crystal directional couplers (PCDCs) are formed by two parallel PCWGs which are placed closely. They are important components in optical integrated circuits. The characteristics of PCDCs, namely the coupling frequency, the coupling length and the insertion loss, are sensitive to the structure parameters of PCDCs, such as the length and width of the waveguide, the radii of air holes in the coupling region, and the ratio of the radii of air holes to the lattice constant, etc. Up to now, a lot of studies have been carried out into PCDCs [5]–[11], including the researches on the relationship between the coupling characteristics and the waveguide length [5]. It was also reported that the coupling length could be changed by adjusting the radii of air holes in the coupling region [6]–[8]. However, the effects of the width of PCWG and the ratio of the radii of air holes to the lattice constant on the coupling length have never been studied. Meanwhile, the performances of PCDCs are deteriorated by the structural deviations accompanied during the fabrication process, such as the size nonuniformity and position misalignment of air holes, etc. [9]–[11]. In this paper, the effects of both structure parameters and structural deviations on the characteristics of PCDCs were analyzed by plane wave expansion (PWE) and finite difference time domain (FDTD) methods. The research results show that the power remaining phenomenon increases the insertion loss of PCDCs, especially for the PCDCs with shorter coupling length. An improved structure, which increases the radii of air holes in the post coupling region, is proposed to suppress the remained power and reduce the insertion loss effectively. Through statistical analyses of the PCDCs with structural deviations, it's found that the air hole position misalignment perpendicular to the waveguide direction has a larger effect on the characteristics of PCDCs than the air hole size nonuniformity and the air hole position misalignment parallel to the waveguide direction, and reducing r/a is helpful to improving the robustness of PCDCs. These researches not only reveal the operation mechanism of PCDCs, but also benefit the design of practical PCDCs greatly.

Manuscript received November 06, 2008; revised February 25, 2009. First published April 28, 2009; current version published August 21, 2009. This work was supported in part by the National Natural Science Foundation of China (NSFC-60537010) and in part by the National Basic Research Program of China (973 Program) under Contracts 2006CB302804 and 2007CB307004.

The authors are with the Department of Electronic Engineering, State Key Laboratory of Integrated Optoelectronics, Tsinghua University, Beijing 100084, China (e-mail: maoxy@mails.tsinghua.edu.cn; yidonghuang@mail.tsinghua.edu.cn; cuiky05@mails.tsinghua.edu.cn; zhangchao02@mails.tsinghua.edu.cn; zwei@mail.tsinghua.edu.cn; pengjd@mail.tsinghua.edu.cn).

Digital Object Identifier 10.1109/JLT.2009.2021865

II. Theory and Results

A. Relationship Between Coupling Characteristics and Structure Parameters

The structure of the PCDC is shown in Fig. 1. Here the PCDC is composed of a triangular lattice of air holes formed in the GaAs-based dielectric slab which is sandwiched by air. To relieve the need for three-dimensional (3D) calculations, the effective refractive index $(n_{\text{eff}} = 2.95)$ has been used to replace the refractive index of the dielectric material [12], [13]. The effective refractive index method has been known as a good approximation to 3D calculations and can reduce the computing time and memory remarkably. By removing two lines of air holes in the $\Gamma - K$ direction, two single-line defect waveguides separated by three lines of air holes are introduced. The lattice constant and the radii of air holes are a and r, respectively. The waveguide width W is the distance between the centers of the two lines of air holes separated by the single-line defect waveguide, and $W_0 = 1.732a$, corresponds to a normal single-line defect

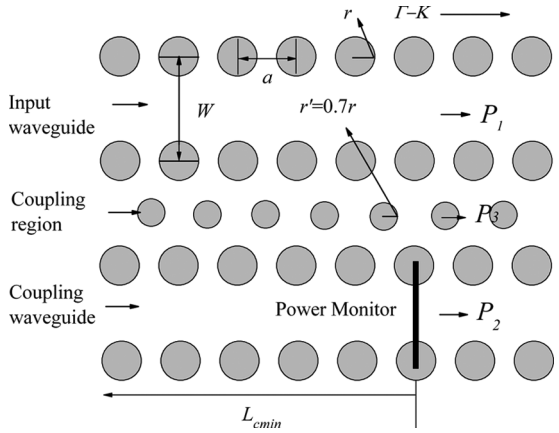

Fig. 1. Structures of the PCDC. The waveguide is along the $\Gamma - K$ direction, and its width is W. The lattice constant is a, and the radii of air holes are r. The radii of air holes in the middle row of the coupling region are represented by r'.

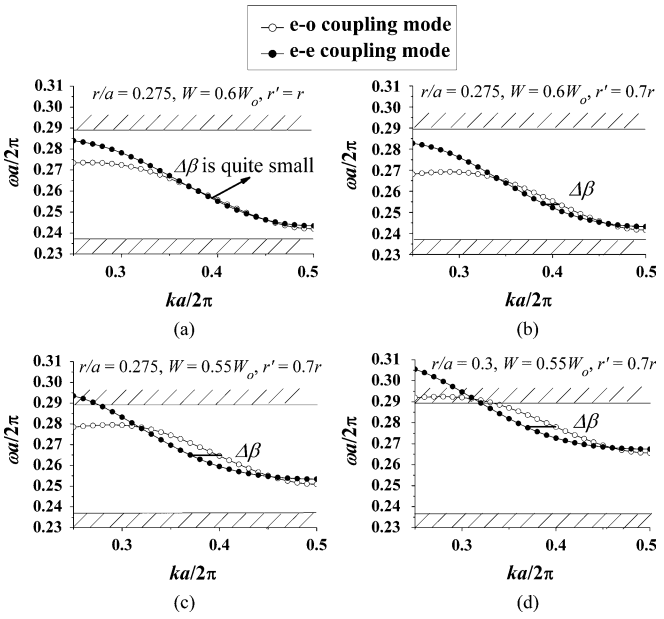

Fig. 2. Dispersion curves of the PCDCs with different structure parameters. The wave vector k is along the $\Gamma - K$ direction: (a) $r/a = 0.275$, $W = 0.6\,W_0$, $r' = r$; (b) $r/a = 0.275$, $W = 0.6\,W_0$, $r' = 0.7r$; (c) $r/a = 0.275$, $W = 0.55\,W_0$, $r' = 0.7r$; (d) $r/a = 0.3$, $W = 0.55\,W_0$, $r' = 0.7r$.

waveguide. The radii of air holes in the coupling region which affect the coupling characteristics greatly are indicated by r'.

The coupling mode theory was employed to analyze the characteristics of PCDCs. Here only TE modes were considered because the structure of etching air holes in the dielectric slab is easy to have a TE band gap [5]. The PCWG usually has two guided modes within the photonic band gap, which are even mode or odd mode because their magnetic field has even or odd symmetry with respect to the mirror plane along the guide axis respectively. Due to the close proximity of the two parallel PCWGs, the mode in the single PCWG will split into two kinds of modes [8], [14]. The even mode splits into even-even (e-e) mode and even-odd (e-o) mode, and the odd mode splits into odd-odd (o-o) mode and odd-even (o-e) mode. Because no odd modes can be stimulated in the PCWG if the incident light has the centre plane of the PCWG for even symmetry, only the even mode was considered in our researches. The e-e and e-o modes have different propagation constants β_{ee} and β_{eo}, respectively, and the mismatch between β_{ee} and β_{eo} determines the coupling length L_c. The larger $\Delta\beta(\Delta\beta = \beta_{ee} - \beta_{eo})$ is, the shorter L_c is, complying with [5]

$$L_c = \frac{\pi}{\beta_{ee} - \beta_{eo}} = \frac{\pi}{\Delta\beta}. \tag{1}$$

Utilizing the PWE method, we calculated the TE band diagrams of PCDCs with different $r/a, W$, and r'. A grid size step of $a/32$ was applied here. Fig. 2 shows the defect modes in the photonic band gap. For a PC structure with $r/a = 0.275$ [Fig. 2(a)–(c)], a TE bandgap appears in the range of normalized frequency 0.237 to 0.289. The e-e mode and e-o mode of PCDCs are originated from the even mode of the single waveguide. In Fig. 2(a), for $W = 0.6\,W_0$, and $r' = r$, it is noticed that there is a wide frequency range in which the mismatch $\Delta\beta$ is quite small. Weak coupling occurs in this frequency range, leading to a very long coupling length. While in Fig. 2(b), where r' is reduced to $0.7r$, $\Delta\beta$ becomes larger than that shown in Fig. 2(a). $\Delta\beta$ becomes further larger when W is also reduced to $0.55\,W_0$ [Fig. 2(c)]. It is noticed that changing dispersion curves, namely the band diagrams, will change $\Delta\beta$, therefore the coupling length and strength will be changed. In PCDCs with enough wide bandgap, the refractive index contrast between the air holes and the slab is usually quite large. This will strongly confine the optical field profiles of guided modes inside the guiding waveguides. As a result, the coupling strength is weak because the overlap of the field profiles is small. Reducing r' and W equals to reducing the refractive index contrast between the waveguides and the coupling region, therefore the confinement of the guided modes is weaken and the coupling strength determined by the overlap of the field profiles of the two guided modes is enhanced. Similar experimental results have been reported in [8], where decreasing r' shortens the coupling length. Fig. 2(d) shows the band diagrams for $r/a = 0.3$, $W = 0.55\,W_0$ and $r' = 0.7r$. Compared to Fig. 2(c), the normalized frequency of the modes in Fig. 2(d) is higher, but $\Delta\beta$ does not change much because larger r/a increases r' and decreases W at the same time.

Coupling lengths of the PCDCs with different structure parameters were calculated by FDTD with perfectly matched layer (PML) absorbing boundary conditions at the boundary of the PCDCs to terminate the computation window [15]. The thickness of PML was $3a$ and the FDTD grid size was set to $a/32$. Fig. 3 shows the normalized coupling lengths of PCDCs with different structures. Line (f), (g), (h) in Fig. 3 were calculated by formula (1) in which $\Delta\beta$ was calculated by the PWE method. It can be seen that line (b), (d), (e) accord with line (f), (g), (h) well, which significantly validates our computations. Comparing the line (a) and (b) or (c) and (d), where r/a and W are the same and only r' is changed from $0.81r$ to $0.7r$, it can be found that a smaller r' corresponds to a shorter coupling length in the whole frequency range. Line (a) and (c) or (b) and (d), where only W is changed from $0.6\,W_0$ to $0.55\,W_0$ with fixed r' and r/a, show a narrower waveguide has a shorter coupling length and a higher coupling frequency. Line (e) has a higher coupling frequency and almost the same coupling length with line (d), which means

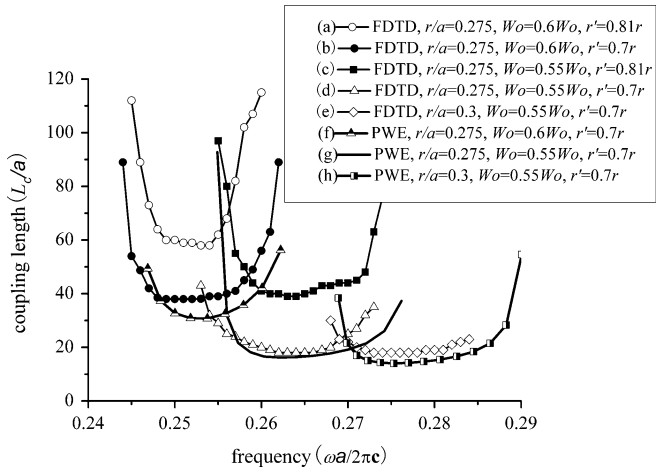

Fig. 3. The coupling lengths of the PCDCs with different structure parameters versus normalized frequency.

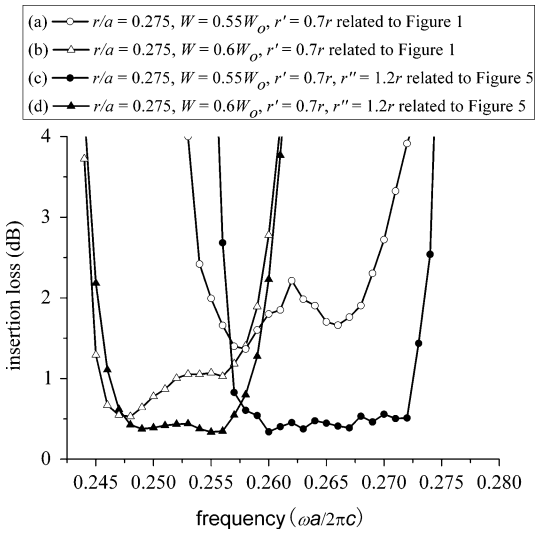

Fig. 4. The insertion loss of two kinds of PCDCs. The insertion loss of the structure of Fig. 1 has been shown by line (a) and (b). The insertion loss of the structure of Fig. 5 has been shown by line (c) and (d).

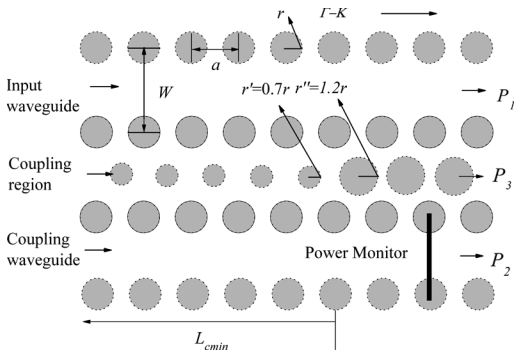

Fig. 5. The structure of the improved PCDCs. The radii of air holes in the post coupling region are r'', and $r'' = 1.2r$.

the coupling length is not very sensitive to r/a. These simulation results match the theoretical analyses of the band diagrams above very well.

Different frequencies correspond to different coupling lengths, and here the shortest coupling length in the whole frequency range is denoted by L_{cmin}. We set the waveguide length to L_{cmin} for each set of structure parameters.

In Fig. 1, a power monitor is set at the waveguide length of L_{cmin} to detect the power in the coupling waveguide. The total output power P is distributed among three areas: the input waveguide with power P_1, the coupling waveguide with power P_2, and the coupling region with power P_3, so $P = P_1 + P_2 + P_3$. We consider the insertion loss as $-10\log(P_2/P)$. The insertion loss of the structure in Fig. 1 has been shown by line (a) and (b) in Fig. 4. It can be seen that the insertion loss is high because of the power remaining phenomenon, described in [16]. Reducing r' and W is equal to reducing the refractive index contrast between the waveguides and the coupling region, which can weaken the confinement of the guided modes and increase the overlap of the field profiles of the two guided modes, therefore there will be more power in the coupling region. This remained power in the coupling region, P_3, strongly affects the characteristics of the PCDCs. On one hand, the more the power in the coupling region is, the stronger the coupling strength and the shorter the coupling length can be obtained (this is why more power leaking into the coupling region by reducing the waveguide width or r' can increase the coupling strength), on the other hand, the more the power in the coupling region is, the lower the density of the power inside the waveguides is. The remained power P_3 can be considered as a waste power because it belongs to neither input waveguide nor coupling waveguide and is difficult to be coupled into the common waveguide which is connected with the PCWG because of mode mismatch. As a result, the insertion losses of PCDCs become larger. This power remaining phenomenon is enhanced when the coupling length becomes shorter, so the insertion loss for lines (a) and (b) in Fig. 4 have a maximum near the frequency 0.262 and 0.253 respectively, which correspond to the shortest coupling length.

In order to depress the remained power in the coupling region, a kind of improved structure was proposed by introducing a post coupling region in the middle row after the waveguide length of L_{cmin}. The radii of air holes in the post coupling region r'' are different from r', as shown in Fig. 5. Simulation was carried out for $r'' = 1.2r$ and the monitor was placed two lattice periods after L_{cmin}. In this structure, the remained power in the post coupling region reduces and transfers into the coupling waveguide quickly within 2 or 3 pitches of air holes because of increasing r''. The insertion loss of the structure in Fig. 5 has been shown by line (c) and (d) in Fig. 4, and is obviously reduced compared with line (a) and (b). Meanwhile, it can be seen that the insertion loss for lines (c) and (d) in Fig. 4, are flat over a large frequency range compared with lines (a) and (b) because of the depressing of the power remaining phenomenon. B.

B. Effects of Structural Deviations on the Characteristics of PCDCs

In Fig. 5, the dot line circles represent the ideal PC structure. In fact, there are always structural deviations from the ideal PC structure because of the fabrication imperfections. We consider the size nonuniformity of these hundreds of air holes in PCDCs as a normal distribution in which the air hole diameter deviations $D - D_0$ (D_0 and D are the diameters of ideal and actual

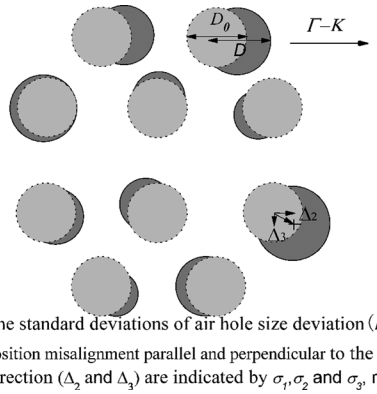

Fig. 6. The instruction of air hole size nonuniformity and position misalignment in PCDCs.

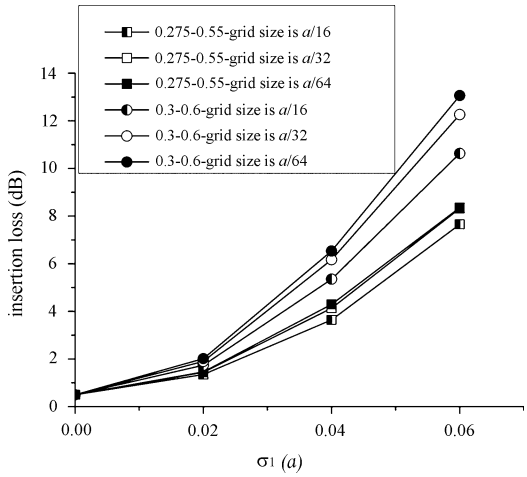

Fig. 7. Simulation results for the insertion loss of PCDCs due to σ_1 with grid size of $a/16, a/32, a/64$. And the structure parameters of the two devices are $r/a = 0.275$, $W = 0.55\ W_0$, $r' = 0.7r$, $r'' = 1.2r$ and $r/a = 0.3$, $W = 0.6\ W_0$, $r' = 0.7r$, $r'' = 1.2r$.

air holes in PCDCs) follow a normal "bell curve" distribution with a standard deviation σ_1. And the standard deviations of the air hole position misalignment parallel and perpendicular to the waveguide direction are indicated by σ_2 and σ_3, respectively, as that shown in Fig. 6 where the solid line circle represents the actual air holes [17]. The probability of air hole diameters complies with formula (2)

$$f(D - D_0) = \frac{1}{\sqrt{2\pi}\sigma_1} \exp\left\{-\frac{(D - D_0)^2}{2\sigma_1^2}\right\} \tag{2}$$

And the probability of air hole position misalignment complies with

$$f(\Delta_2) = \frac{1}{\sqrt{2\pi}\sigma_2} \exp\left\{-\frac{\Delta_2^2}{2\sigma_2^2}\right\} \tag{3}$$

$$f(\Delta_3) = \frac{1}{\sqrt{2\pi}\sigma_3} \exp\left\{-\frac{\Delta_3^2}{2\sigma_3^2}\right\} \tag{4}$$

where Δ_2, Δ_3 are the air hole position misalignment parallel and perpendicular to the waveguide.

The deterioration of the insertion loss of PCDCs due to σ_1, σ_2 and σ_3 was simulated by FDTD method with different r/a and waveguide width W. The waveguide length was L_{cmin} for different r/a and W. The σ_1, σ_2 and σ_3 of the fluctuation patterns were 0, $0.02a$, $0.04a$, $0.06a$ and for each value of σ_1, σ_2 and σ_3, 10 fluctuation patterns were used to get a statistical result. The FDTD parameters except the grid size were the same with those used in the FDTD simulation of coupling length in Fig. 3. In order to estimate the influences of FDTD grid size on the calculation results, we first calculated various σ_1 for two perturbed devices with the grid size of $a/16$, $a/32$, $a/64$, respectively, as shown in Fig. 7. The structure parameters of the two devices are $r/a = 0.275$, $W = 0.55\ W_0$, $r' = 0.7r$, $r'' = 1.2r$, and $r/a = 0.3$, $W = 0.6\ W_0$, $r' = 0.7r$, $r'' = 1.2r$, respectively. It can be seen that the main tendency of the insertion loss is almost the same, and the calculation results converge when the grid size becomes smaller and smaller.

As a further smaller grid size corresponds to a further longer calculation time, a grid size of $a/64$ was used in the FDTD method and a FDTD stop time of 1000 was applied in this paper. The results are shown in Fig. 8. We can see that when σ_1, σ_2 or σ_3, is larger than $0.02a$ (that is about 9 nm for $a = 450$ nm), the insertion loss will increase dramatically, which means it's important to control the standard deviation of structural fluctuations within 9 nm during the fabrication process, that is, the structural fluctuations of most air holes should be controlled in the range from -9 nm to 9 nm. This fabrication precision can be realized by current advanced electron beam lithography (EBL) which can make 10 nm or even smaller line width. It also can be found that σ_3 has a larger effect on the insertion loss of PCDCs than σ_1 and σ_2 in the case that the structure parameters are the same. It means the insertion loss of PCDCs are more sensitive to the air hole position perpendicular to the waveguide direction. Meanwhile the results show that $r/a = 0.275$ has a smaller insertion loss than $r/a = 0.3$ when they have the same σ_1, σ_2 or σ_3. That means a small r/a is helpful to improving the robustness of PCDCs. These conclusions will benefit the design and fabrication of practical PCDCs greatly.

III. Conclusions

We have studied the effects of structure parameters and structural deviations on the characteristics of PCDCs theoretically. It is found that reducing the waveguide width and decreasing the radii of air holes in the coupling region can shorten the coupling length of PCDCs effectively. While a shorter coupling length, accompanying by a strong coupling strength, would lead to an increasing density of power remained in the coupling region, so called mode power remaining phenomenon. This phenomenon is detrimental to reducing the insertion loss of PCDCs. An improved structure was proposed by simply increasing the radii of air holes in the post coupling region. The simulation results demonstrated that the insertion loss can be reduced dramatically by suppressing the power remaining phenomenon. The statistical analyses of PCDCs containing structural deviations have been carried out. The results show that when σ_1, σ_2 or σ_3, is larger than $0.02a$ (that is about 9 nm for $a = 450$ nm), the insertion loss will increase dramatically and σ_3 has a larger effect on the insertion loss of PCDCs than σ_1 and σ_2. Meanwhile reducing r/a is helpful to improving the robustness of PCDCs.

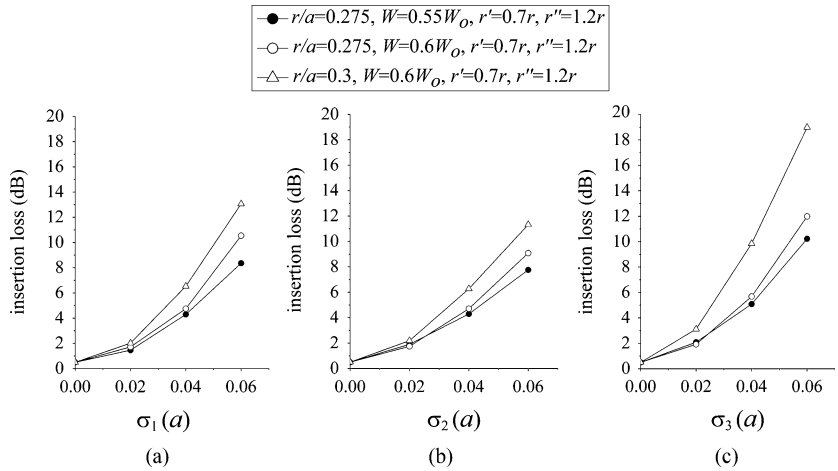

Fig. 8. Simulation results for the insertion loss of PCDCs with different structure parameters due to σ_1, σ_2 or σ_3.

These works are significant in the design and fabrication of practical PCDCs.

REFERENCES

[1] A. Chutinan and S. Noda, "Waveguides and waveguide bends in two-dimensional photonic crystal slabs," *Phys. Rev. B*, vol. 62, pp. 4488–4492, Aug. 2000.

[2] J. S. Jensena and O. Sigmund, "Systematic design of photonic crystal structures using topology optimization: Low-loss waveguide bends," *Appl. Phys. Lett.*, vol. 84, pp. 2022–2024, Mar. 2004.

[3] M. Notomi, A. Shinya, S. Mitsugi, E. Kuramochi, and H. Y. Ryu, "Waveguides, resonators and their coupled elements in photonic crystal slabs," *Opt. Exp.*, vol. 12, pp. 1551–1561, Apr. 2004.

[4] H. Nakamura1 *et al.*, "Ultra-fast photonic crystal/quantum dot alloptical switch for future photonic networks," *Opt. Exp.*, vol. 12, pp. 6606–6614, Nov. 2004.

[5] Y. Tanaka *et al.*, "Coupling properties in a 2-D photonic crystal slab directional coupler with a triangular lattice of air holes," *IEEE J. Quant. Electron.*, vol. 41, pp. 76–84, Jan. 2005.

[6] M. Soltani, A. Adibi, Y. Xu, and R. Lee, "Systematic design of directional couplers in photonic crystal," *Lasers Electro-Optics*, pp. 944–946, Jun. 2003.

[7] A. Martinez, F. Cuesta, and J. Marti, "Ultrashort 2-D photonic crystal directional couplers," *Photon. Technol. Lett.*, vol. 15, pp. 694–696, May 2003.

[8] D. M. Pustai *et al.*, "Characterization and analysis of photonic crystal coupled waveguides," *J. Microlithogr. Microfab., Microsyst.*, pp. 292–299, Oct. 2003.

[9] A. F. Koenderink *et al.*, "Optical extinction due to intrinsic structural variations of photonic crystals," *Phys. Rev. B*, vol. 72, p. 153102, Jan. 2005.

[10] T. Kamalakis *et al.*, "Numerical study of the implications of size nonuniformities in the performance of photonic crystal couplers using coupled mode theory," *J. Quant. Electron.*, vol. 41, pp. 863–871, Jun. 2005.

[11] S. Lan *et al.*, "Similar role of waveguide bends in photonic crystal and disordered defects in coupled cavity waveguides: Problem in realizing photonic crystal circuits," *Phys. Rev. B*, vol. 67, no. 7, p. 115208, Mar. 2003.

[12] M. Qiu, "Effective index method for heterostructure-slab-waveguide-based two-dimensional photonic crystals," *Appl. Phys. Lett.*, vol. 81, pp. 1163–1165, Aug. 2002.

[13] A. Adibi *et al.*, "Design of photonic crystal optical waveguides with single mode propagation in the photonic bandgap," *Electron. Lett.*, vol. 36, pp. 1376–1378, Aug. 2000.

[14] S. Kuchinsky *et al.*, "Coupling between photonic crystal waveguides," *J. Quant. Electron.*, vol. 38, pp. 1349–1352, Oct. 2002.

[15] M. Koshiba *et al.*, "High-performance absorbing boundary conditions for photonic crystal waveguide simulations," *IEEE Microw. Wireless Compon. Lett.*, vol. 11, pp. 152–154, Apr. 2001.

[16] X. Y. Mao *et al.*, "Reducing insertion loss of photonic crystal couplers by suppressing the remained power," *Chinese Phys. Lett.*, vol. 24, pp. 454–457, Feb. 2007.

[17] M. Y. Shih *et al.*, "Statistical analyses of 2D photonic bandgap waveguides containing structural deviations," *Proc. SPIE*, vol. 5000, pp. 51–57, Jul. 2003.

Xiaoyu Mao received the B.S. degree in electronic and engineering from Tsinghua University, Beijing, China, in 2005, where he is currently working toward the Ph.D. degree.

His recent research interest is in photonic crystal slab fabricated by semiconductor technology.

Yidong Huang (M'98) received the B.S. and Ph.D. degrees in optoelectronics from Tsinghua University, Beijing, China, in 1988 and 1994, respectively.

From 1991 to 1993, she was with Arai Laboratories, Tokyo Institute of Technology, Tokyo, Japan, on leave from the Tsinghua University. She was with the Photonic and Wireless Devices Research Laboratories, NEC Corporation, from 1994 to 2003, where she was engaged in the research on semiconductor laser diodes for optical-fiber communication. In 2003, she joined the Department of Electronics Engineering, Tsinghua University, as a Professor. She is presently engaged in research on nano-structure optoelectronics.

Kaiyu Cui was born in Jilin Province, China, on April 11, 1982. She received the B.S. degree in electronic engineering from Jilin University, Changchun, China, in 2005. She is currently working toward the Ph.D. degree at Tsinghua University, Beijing, China.

Her current research interest is in the area of two-dimensional active photonic crystal devices.

Chao Zhang received the B.S. degree in electronic engineering from Tsinghua University, Beijing, China, where he is working toward the M.S. degree.

His current research object is silicon waveguide devices, especially slow light in photonic crystal waveguide.

Wei Zhang received the B.S. and Ph.D. degrees in electronic engineering from Tsinghua University, Beijing, China, in 1998 and 2003, respectively.

In 2003, he joined the Department of Electronics Engineering, Tsinghua University, where he is currently an Associate Professor. His major research interests include active and passive fiber device, microstructure optoelectrical materials, especially microstructure fibers, and their applications.

Jiangde Peng graduated from Tsinghua University, Beijing, China, in 1964.

Since 2004, he has been with the Department of Electronic Engineering, Tsinghua University, where he is currently a Professor. He was a Senior Visiting Scholar in the CNRS Laboratoire de Photophysique Moleculare, Universite d'Orsay, France, from 1973 to 1975, and the Department of EE-Systems, University of Southern California, from 1997 to 1998. He has been engaged in research on active and passive fiber devices for WDM optical fiber communications, with specific emphasis on fiber amplifiers and lasers. At present, his primary interests focus on slow light, entangled photon-pair sources and sensors based on micro- nano-structure materials. He is the author or coauthor of over 100 papers, 12 patents and one textbook: entitled *Fundamentals of Optoelectronic Technologies*.

Jiangde Peng is a member of the Optical Society of China and SPIE. He received the National Invention Award in 1997.